WATER RESEARCH 44 (2010) 1104–1113

Available at www.sciencedirect.com

ScienceDirect

journal homepage: www.elsevier.com/locate/watres

Influence of organic matter on the transport of *Cryptosporidium parvum* oocysts in a ferric oxyhydroxide-coated quartz sand saturated porous medium

R.A. Abudalo[a], J.N. Ryan[a,*], R.W. Harvey[b], D.W. Metge[b], L. Landkamer[b]

[a] 428 UCB, Department of Civil, Environmental, and Architectural Engineering, University of Colorado, Boulder, CO 80309, USA
[b] U.S. Geological Survey, National Research Program, 3215 Marine Street, Boulder, CO 80304, USA

ARTICLE INFO

Article history:
Received 23 May 2009
Received in revised form
8 September 2009
Accepted 17 September 2009
Available online 22 September 2009

Keywords:
Cryptosporidium parvum
Oocyst
Transport
Organic matter
Ferric oxyhydroxide
Zeta potential

ABSTRACT

To assess the effect of organic matter on the transport of *Cryptosporidium parvum* oocysts in a geochemically heterogeneous saturated porous medium, we measured the breakthrough and collision efficiencies of oocysts as a function of dissolved organic matter concentration in a flow-through column containing ferric oxyhydroxide-coated sand. We characterized the surface properties of the oocysts and ferric oxyhydroxide-coated sand using microelectrophoresis and streaming potential, respectively, and the amount of organic matter adsorbed on the ferric oxyhydroxide-coated sand as a function of the concentration of dissolved organic matter (a fulvic acid isolated from Florida Everglades water). The dissolved organic matter had no significant effect on the zeta potential of the oocysts. Low concentrations of dissolved organic matter were responsible for reversing the charge of the ferric oxyhydroxide-coated sand surface from positive to negative. The charge reversal and accumulation of negative charge on the ferric oxyhydroxide-coated sand led to increases in oocyst breakthrough and decreases in oocyst collision efficiency with increasing dissolved organic matter concentration. The increase in dissolved organic matter concentration from 0 to 20 mg L^{-1} resulted in a two-fold decrease in the collision efficiency.

1. Introduction

Contamination of drinking water by pathogenic microbes – viruses, bacteria, and protozoa – is considered as one of the most important water supply problems of our day. Current concern is focused on *Cryptosporidium parvum*, a protozoan parasite that moves from host to host as an oocyst (Carey et al., 2004). An outbreak of *Cryptosporidium parvum* caused the death of over 100 citizens of Milwaukee, Wisconsin, in 1993 (MacKenzie et al., 1994). Water utilities are increasingly using bank filtration to remove microbes from surface water supplies and to reduce the need for disinfection (Tufenkji et al., 2002; Gollnitz et al., 2003). Bank filtration uses alluvial aquifer sediments to filter microbes from river water. The effectiveness of microbe removal by bank filtration removal depends on the characteristics of the pumping-induced groundwater flow, the alluvial sediments, and the solution chemistry. Removal can be difficult to predict because of physical and geochemical heterogeneity of the alluvial sediments and the pore waters.

One form of geochemical heterogeneity in alluvial aquifers that affects microbe removal is the nature and abundance of organic matter. Organic matter is present in the sediments as lignin, proteins, kerogen, and black carbon derived from

---

[*] *Corresponding author*. Tel.: +1 303 492 0772.

E-mail addresses: rula_abudalo@yahoo.com (R.A. Abudalo), joseph.ryan@colorado.edu (J.N. Ryan), rwharvey@usgs.gov (R.W. Harvey), dwmetge@usgs.gov (D.W. Metge), llandkam@mines.edu (L. Landkamer).

0043-1354/$ – see front matter © 2009 Elsevier Ltd. All rights reserved.
doi:10.1016/j.watres.2009.09.039

terrestrial plants in discrete phases and mineral coatings at concentrations ranging up to a few percent. In the pore waters, organic matter is present as dissolved humic substances and organic acids of lower molecular weight at concentrations up to a few milligrams of carbon per liter. During bank filtration, the nature and abundance of dissolved organic matter is altered by a variety of biological processes and sorption (Miettinen et al., 1994; Cosovic et al., 1996; Grünheid et al., 2005).

In aquifer sediments, minerals like ferric and aluminum oxyhydroxides and clay edges are typically coated by organic matter (Amelung et al., 2002; Wagai et al., 2009). These minerals often form patchy coatings and interstitial aggregates on primary mineral grains (Ryan and Gschwend, 1992; Coston et al., 1995; Penn et al., 2003). Ferric and aluminum oxyhydroxides and clay edges are amphoteric minerals with relatively high points of zero charge (pH_{pzc}). Typical groundwater pH values are below their pH_{pzc} values; therefore, these minerals adsorb protons and acquire positive surface charge. At typical groundwater pH values, most pathogenic microbes – viruses, bacteria, protozoa – are negatively-charged. Positively-charged surfaces effectively remove negatively-charged colloids (Song et al., 1994; Johnson et al., 1996) and microbes (Scholl and Harvey, 1992; Mills et al., 1994; Zhuang and Jin, 2003b; Abudalo et al., 2005; Foppen and Schijven, 2005; Hijnen et al., 2005; Kim et al., 2008) from passing pore waters. Positively-charged surfaces also effectively adsorb organic matter (Davis, 1982; Gu et al., 1994), which is mainly anionic at typical groundwater pH values, and the adsorption of sufficient organic matter is presumed to be capable of reversing the surface charge of the ferric and aluminum oxyhydroxide coatings from positive to negative.

If organic matter adsorption can reverse the surface charge of aquifer grains, then organic matter should inhibit the removal of negatively-charged colloids and microbes. Most research, in the laboratory and in the field, shows this is true for colloids (Amirbahman and Olson, 1993; Kretzschmar et al., 1995; Ryan et al., 1999; Franchi and O'Melia, 2003), viruses (Fuhs et al., 1985; Powelson et al., 1990; Pieper et al., 1997; Zhuang and Jin, 2003a; Levy et al., 2007; Yuan et al., 2008), bacteria (Martin et al., 1991; Johnson and Logan, 1996; Dong et al., 2002; Hall et al., 2005), and oocysts (Dai and Hozalski, 2002, 2003). Inhibition of removal was mainly attributed to blocking of colloid and microbe attachment by organic matter adsorption on the porous medium, but some researchers attributed inhibition of removal to an increase in the negative surface charge of microbes caused by adsorption of organic matter to the microbe surfaces (Bixby and O'Brien, 1979; Dai and Hozalski, 2002, 2003). Adsorption of organic matter to microbes has been measured directly by a variety of methods (Bixby and O'Brien, 1979; Campbell et al., 1997; Fein et al., 1999; Parent and Velegol, 2004) or indirectly by an increase in negative zeta potential (Dai and Hozalski, 2002, 2003). In contrast, Liu et al. (2009) found that organic matter enhanced the removal of some *Cryptosporidium parvum* oocysts to organic matter-coated silica surfaces; they attributed this behavior to surface charge heterogeneity and the presence of positively-charged area on the organic matter-coated surface.

The goal of this research is to examine the influence of organic matter on the transport of *Cryptosporidium parvum* oocysts through a ferric oxyhydroxide-coated quartz sand saturated porous medium and to ascertain the mechanism by which organic matter affects oocyst removal. To do this, we measured the effect of different concentrations of dissolved organic matter on the streaming potential of the porous medium and the zeta potential of the oocysts.

2. Materials and methods

2.1. *Cryptosporidium parvum* oocysts

Formalin-inactivated *Cryptosporidium parvum* oocysts were obtained from Sterling Parasitology Laboratory (SPL) at the University of Arizona at Tucson. We used formalin-inactivated oocysts in these experiments even though inactivation results in changes to oocyst deposition behavior (Kuznar and Elimelech, 2005) because we used formalin-inactivated oocysts in an intermediate-scale aquifer tank experiment in a laboratory that could not be secured for the use of active oocysts. The oocysts were shed from a calf infected with the Iowa isolate of *Cryptosporidium parvum*, purified at SPL by discontinuous sucrose and cesium chloride centrifugation gradients (Brush et al., 1998), re-suspended in a solution of 5% formaldehyde, 0.01% Tween 20, 0.85% NaCl, and three antibiotics (penicillin, 111 U mL^{-1}; streptomycin, 111 U mL^{-1}; gentamicin, 56 $\mu g\ mL^{-1}$), and stored at 4 °C. The oocysts were pelleted from the formalin solution by centrifugation (12,000 × *g*, 4 °C, 30 min) and re-suspended in the experimental solution (10^{-4} M NaCl, pH 5.6–5.8) at a concentration of about 10^5 oocysts per milliliter for at least 2 weeks before the column transport experiments.

The oocysts were enumerated by epifluorescence microscopy. Samples containing oocysts were stained with DAPI (4,6-diamidino-2-phenylindole; 0.1 mg L^{-1}) for 15 min and filtered with vacuum assistance (0.34 bar) onto black polycarbonate membranes (1.0 μm pore diameter, GE Osmonics) overlaying nitrocellulose backing filters (0.45 μm pore diameter, Pall–Gelman). The membranes were mounted on glass slides and the oocysts were counted manually using an epifluorescence microscope (Nikon Optiphot-2, 788× magnification, 350 nm excitation, 470 nm emission). At least 20 fields of view with 10 oocysts per field, or a maximum of 50 fields with fewer than 10 oocysts per field, were counted.

The average diameter of the DAPI-stained oocysts was measured by flow cytometry and epifluorescence microscopy outfitted with image analysis (Image Technology Corporation, Deer Park, NY). Fluorescent polystyrene microspheres (0.2–6.0 μm; Polysciences) were used to calibrate both the flow cytometer (Biorad, HS Bryte) and the epifluorescence microscopy image analysis.

The buoyant density of the oocysts was determined by density gradient centrifugation in Percoll I solution (1.131 g mL^{-1}, Sigma Chemical Co.) following a procedure used by Harvey et al. (1997). The gradients were overlaid with 500 μL of an oocyst suspension at a concentration of about 1×10^7 oocyst mL^{-1} and density marker beads (synthetically derived from the polysaccharide dextran; Sigma Chemical Co.) in a range of 1.095–1.138 g mL^{-1} prepared in 0.15 M NaCl. The gradient was developed by centrifugation

(15,000 × *g*, 30 min, 20 °C) and allowed to come to a standstill without braking.

The electrophoretic mobility of the oocysts was measured by laser Doppler microelectrophoresis (Particle Sizing Systems, 380 ZLS). Oocyst suspensions of about 1×10^6 oocyst mL^{-1} concentration were prepared in a 1×10^{-4} M NaCl solution at pH 5.6–5.8 containing a range of dissolved organic matter concentrations (0–19.2 mg L^{-1}). For each dissolved organic matter concentration, three replicate measurements were made. Electrophoretic mobility was converted to zeta potential using the Smoluchowski equation (Elimelech et al., 1995).

2.2. Dissolved organic matter

The dissolved organic matter (DOM) used in these experiments is a fulvic acid fraction isolated from water collected from a eutrophic marshland dominated by cattails in the northern Florida Everglades (the F1 site, Water Conservation Area 2; Ravichandran et al., 1998). The fulvic acid fraction was isolated in the hydrogen-saturated form by filtration (0.45 μm silver membrane), XAD-8 resin chromatography, and freeze-drying (Aiken et al., 1992). This fulvic acid is not broadly representative of dissolved organic matter in the subsurface environment, but it was available in sufficient quantities and well-characterized. Some key characteristics of this fulvic acid include a molecular weight of 850 Da measured by high-pressure size exclusion chromatography, an acidic group density of 6.9 meq g^{-1} (carboxylic, 5.6 meq g^{-1}; phenolic, 1.3 meq g^{-1}) measured by acidimetric titration, an aromatic carbon content of 20.1% measured by ^{13}C-nuclear magnetic resonance, a specific ultraviolet (254 nm) absorption of 0.042 L $(mg\ C)^{-1}$ cm^{-1}, and an ash content of 3.2% (Ravichandran et al., 1998).

2.3. Porous media

Well-rounded quartz sand was obtained from a commercial supplier (Unimin Corp., type 2095) and mechanically dry-sieved (+20/−18 mesh) to retain a narrow size fraction (0.84–1.00 mm). To remove surface impurities that might have affected microorganism attachment, the sand fractions were acid-washed by soaking in 12 N HCl for 24 h, rinsed with deionized water until the pH of the rinse water matched that of the deionized water, and baked at 500 °C for 8 h (Redman et al., 1997).

Some of the quartz sand was coated with ferric oxyhydroxide following a previously described procedure (Mills et al., 1994). Sand was added to a solution of 0.28 M $FeCl_3$ on a shaker table, the pH was titrated to about 7.0 by addition of 0.5 M NaOH solution, and the slurry was shaken for 24 h. The coating solution was decanted and the sand was rinsed with deionized water and dried at 90 °C for 24 h. Examination of individual coated grains by thin sectioning and scanning electron microscopy (back-scatter electron detection) showed that 75 ± 5% of the grain surfaces were covered by a relatively uniform layer of iron oxyhydroxide (Abudalo et al., 2005). To create the geochemically heterogeneous porous media, portions of the coated and uncoated sand were mixed to achieve a ferric oxyhydroxide coating surface coverage of 4.0%. The 75% surface coating fraction of the coated grains was accounted for in the mixing.

Streaming potentials (mV) of the ferric oxyhydroxide-coated sand grains were measured by using a streaming potential analyzer (Brookhaven Instrument Corp., BI-EKA). The analyzer was equipped with a cylindrical cell and Ag–AgCl electrodes. The ferric oxyhydroxide-coated sand grains (25 g) were wet-packed in the cylindrical cell in 1×10^{-4} M NaCl solution containing various dissolved organic matter concentrations (0–17.3 mg L^{-1}) at pH 5.6–5.8. This solution (500 mL) was circulated in alternate directions through the cell until equilibrium was reached with respect to specific conductance, pH, and temperature (measured by the streaming potential analyzer) and dissolved organic matter concentration (measured by absorbance of ultraviolet light at 254 nm wavelength and calibrated to dissolved organic matter concentrations). At equilibrium, streaming potential was measured. For each dissolved organic matter concentration, streaming potentials were measured for two replicates with fresh sand and dissolved organic matter solution. Zeta potential was calculated from streaming potential using the Helmholtz–Smoluchowski equation (Johnson, 1999).

2.4. Solutions

All solutions were prepared using high-purity water (greater than 18 MΩ cm resistivity; Millipore, Milli-Q). The experimental solutions contained sodium chloride (1×10^{-4} M) and fulvic acid (0–20 mg L^{-1}). The pH of the background solution was adjusted to pH 5.6–5.8 using a 0.01 M sodium hydroxide solution. For column experiments, sodium nitrate (2.5×10^{-3} M) was used as a conservative tracer and measured by ultraviolet absorption (220-nm wavelength) using a spectrophotometer (Spectronic/Unicam, Genesys 10).

2.5. Flow-through column

The transport experiments were conducted in a glass chromatography column (1.5 cm diameter, 10.0 cm length) with polytetrafluoroethene end caps and polypropylene mesh (105 μm openings) on both ends of the column. Columns were packed by adding the 4.0% ferric oxyhydroxide-coated sand to about 1–2 cm of the experimental solution in the column in 1 cm lifts. The column was tapped during the filling procedure to avoid trapping of air bubbles and to promote consistent packing. The filled columns contained about 29 g of sand. The average porosity was 0.38 and the average pore volume was 6.7 mL.

Experimental solutions were injected into the column as 5.0 mL pulses using a high-pressure liquid chromatography stainless steel injector and injection loop (Supelco Rheodyne model 7725). Solutions were pumped through polypropylene tubing and the column using a syringe pump (Isco 500D, stainless steel, 500 mL volume). The experimental pumping rate was set to produce a constant pore velocity of 2.0 ± 0.1 m d^{-1}. Column effluent samples (20–25 samples, 3 mL) were collected on a fraction collector. All experiments were conducted at the ambient laboratory temperature of 20 ± 1 °C.

2.6. Experimental procedures

Before each experiment, the freshly packed column was conditioned with at least 20 pore volumes of background solution and 5.0 pore volumes (33.5 mL) of dissolved organic matter solution (1–20 mg L^{-1} Everglades fulvic acid, 1×10^{-4} M NaCl, pH 5.6–5.8). The ferric oxyhydroxide coatings in the column were exposed to equal amounts of dissolved organic matter as the ferric oxyhydroxide coatings in the streaming potential cells.

For the transport experiments, the tracer solution (2.5×10^{-3} M $NaNO_3$, pH 5.6–5.8) and the oocyst suspensions (4×10^5 oocysts mL^{-1}, 1×10^{-4} M NaCl, 0–20 mg L^{-1} Everglades fulvic acid, pH 5.6–5.8) were injected as separate pulses of 5.0 mL volume to allow the use of a tracer concentration greater than the desired ionic strength for the oocyst transport experiments. For the injections including dissolved organic matter, the injections immediately followed the conditioning of the column with the dissolved organic matter solution and they were followed with the dissolved organic matter solution. The tracer and oocyst breakthroughs were monitored for at least three pore volumes in each experiment. Some of the oocyst transport experiments were conducted in duplicate.

2.7. Breakthrough analysis

Oocyst breakthrough data were used to determine the oocyst collision efficiency (α):

$$\alpha = -\frac{2}{3}\frac{d_g \ln B}{(1-f)L\eta_0} \tag{1}$$

where d_g is the collector grain diameter, B is the ratio of the total number of oocysts breaking through the column to the total number of oocysts injected, f is the porosity, L is the column length, and η_0 is the theoretical single collector efficiency (Harvey and Garabedian, 1991). The single collector efficiency was calculated using the Tufenkji and Elimelech (2004) equations with the parameters listed in Table 1. This determination of the collision efficiency is valid for microorganism removal solely by physicochemical filtration under clean-bed conditions.

3. Results

3.1. Oocyst characteristics

The average oocysts diameter was 3.6 ± 0.3 μm (±one standard deviation) by flow cytometry and 3.8 ± 0.2 μm by microscopy and image analysis. Kuznar and Elimelech (2005) measured a similar diameter (3.7 μm) by microscopy and image analysis for oocysts obtained from the same source. The buoyant density of the oocysts was measured as 1.075 ± 0.005 g cm^{-3} by density gradient centrifugation. Medema et al. (1998) obtained a density of 1.045 g cm^{-3} for oocysts.

The laser Doppler microelectrophoresis measurements of zeta potential of the oocysts as a function of dissolved organic matter concentration revealed no significant change in zeta potential for an increase in dissolved organic matter concentration from 0 to 19.2 mg L^{-1} at a pH of 5.6–5.8 (Fig. 1).

Table 1 – Parameters used in the calculation of the single collector efficiency (η_0) and the collision efficiency (α) for *Cryptosporidium parvum* oocysts.

Parameter	Values
Grain diameter (mm)	0.92
Porosity	0.38
Oocyst diameter (μm)	3.6
Oocyst density (g cm^{-3})	1.075
Fluid approach velocity[a] (m d^{-1})	0.76
Fluid density (g cm^{-3})	0.998
Fluid viscosity (kg m^{-1} s^{-1})	9.8×10^{-4}
Hamaker constant[b] (J)	6.5×10^{-21}
Column length (cm)	10.0

a The approach velocity was calculated as the product of the pore velocity (2.0 m d^{-1}) and the porosity.
b This Hamaker constant value was used by Kuznar and Elimelech (2005) for oocysts.

3.2. Organic matter interaction with the ferric oxyhydroxide-coated quartz sand

The streaming potential measurements of zeta potential of the ferric oxyhydroxide-coated quartz sand (75% ferric oxyhydroxide surface coverage) as a function of dissolved organic matter concentration revealed a decrease in the zeta potential as dissolved organic matter concentration increased from 0 to 17.3 mg L^{-1} (Fig. 1). A reversal of the zeta potential from positive to negative occurred between the dissolved organic matter concentrations of 0 and 1.9 mg L^{-1}.

The amount of adsorbed organic matter increased as the concentration of dissolved organic matter increased (Table 2).

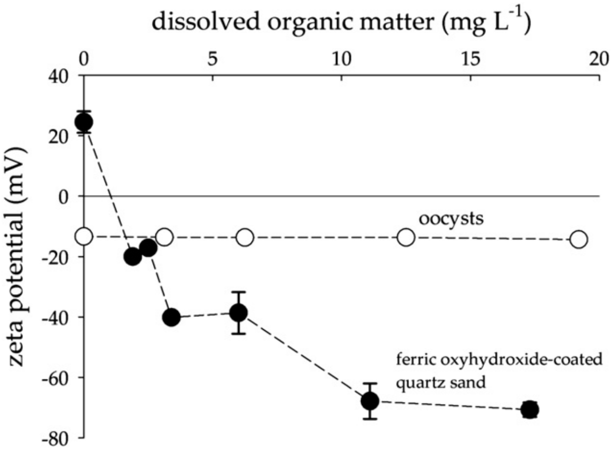

Fig. 1 – Zeta potentials as a function of dissolved organic matter (Everglades fulvic acid) concentrations for formalin-inactivated *Cryptosporidium parvum* oocysts and the ferric oxyhydroxide-coated quartz sand (75 ± 5% surface coverage) in a 10^{-4} M NaCl solution at pH 5.6–5.8 as measured by laser Doppler microelectrophoresis and streaming potential, respectively. Error bars represent one standard deviation for three replicate measurements for the oocysts and for duplicate measurements for the sand.

The amount of organic matter adsorbed on the ferric oxyhydroxide-coated sand was calculated as the difference between the mass of dissolved organic matter in the streaming potential solution divided by the mass of the sand grains or the estimated surface area of the ferric oxyhydroxide coatings. The surface area of the ferric oxyhydroxide coatings was estimated using a measured added iron content of 440 mg kg^{-1} (Abudalo et al., 2005) and an assumed surface area of 50 m^2 g^{-1}, a typical surface area for ferric oxyhydroxide minerals like goethite (Schwertmann and Cornell, 2003). We assumed the surface area of the ferric oxyhydroxide coatings because we have not been able to measure (by nitrogen adsorption) a significant difference in surface area between coated and uncoated quartz grains. Measurement of the amount of dissolved organic matter adsorption by ultraviolet light absorption may bias the measurement because the more aromatic fraction of dissolved organic matter that absorbs ultraviolet light well also preferentially adsorbed to mineral surfaces (Meier et al., 1999). A Langmuir isotherm adequately described the adsorption data with an equilibrium constant of 0.14 ± 0.06 L mg^{-1} and a maximum adsorption density of 1.1 ± 0.2 mg m^{-2} (Fig. 2a). The decrease in the zeta potential of the ferric oxyhydroxide-coated sand correlated well with the increase in the adsorbed organic matter density (Fig. 2b).

3.3. *Oocyst breakthrough curves*

Oocyst breakthrough increased as the dissolved organic matter concentration increased (Fig. 3; one of the duplicate experiments for each dissolved organic concentration is shown). The increase in dissolved organic matter concentration from 0 to 20.0 mg L^{-1} resulted in a 66% increase in the relative breakthrough of oocysts. As the dissolved organic matter increased, the corresponding collision efficiencies decreased by nearly a factor of two, from an α value of 0.26 to 0.12. At all concentrations of dissolved organic matter, the breakthrough of the oocysts coincided closely with the breakthrough of the nitrate tracer. The release of oocysts after the passing of the injected oocysts, or tailing, was observed for oocyst injections with dissolved organic matter. The amount of tailing increased slightly with increasing organic matter concentration.

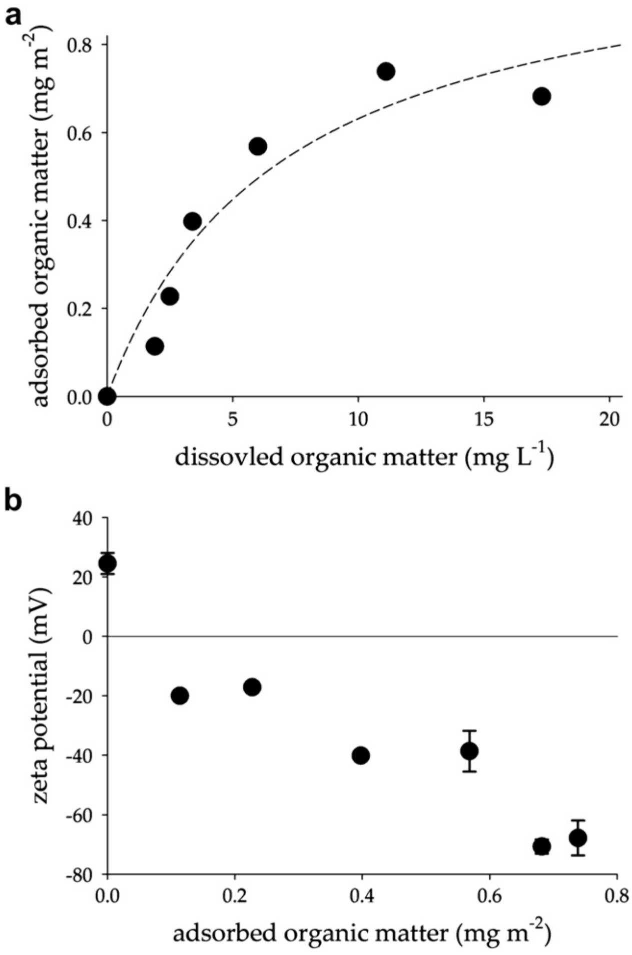

Fig. 2 – Adsorption of dissolved organic matter onto the ferric oxyhydroxide-coated sand (75 ± 5% surface coverage) in the streaming potential cell: (a) adsorbed organic matter density as a function of dissolved organic matter concentration with a Langmuir isotherm; and (b) zeta potential from streaming potential measurement as a function of adsorbed organic matter density. The adsorbed organic matter densities were calculated assuming that the surface area of the ferric oxyhydroxide coating is 50 m^2 g^{-1}.

Table 2 – Amount of dissolved organic matter (DOM; Florida Everglades F1 fulvic acid) adsorbed to the ferric oxyhydroxide-coated sand (FeOx) during the streaming potential measurements.

Initial [DOM] (mg L^{-1})	Equilibrium [DOM] (mg L^{-1})	Adsorbed DOM per mass of sand (mg DOM (kg sand)$^{-1}$)	Adsorbed DOM per surface area of ferric oxyhydroxide coating (mg DOM (m^2 FeOx)$^{-1}$)
0	0	0	0
1.9	1.7	4	0.11
2.5	2.1	8	0.22
3.6	2.9	14	0.40
6.2	5.2	20	0.57
11.1	9.8	26	0.74
17.3	16.1	24	0.68

The adsorbed organic matter concentrations were calculated as the difference in the mass of initial and equilibrium dissolved organic matter (as determined by absorption of ultraviolet light at 254 nm) divided by: (1) the mass of sand in the streaming potential cell (25.0 g); and (2) the estimated surface area of the ferric oxyhydroxide coating in the cell (assuming a surface area of 50 m^2 g^{-1} for the ferric oxyhydroxide coating).

4. Discussion

4.1. *Effect of dissolved organic matter on oocyst surface properties*

The zeta potential we measured for *Cryptosporidium parvum* oocysts inactivated by formalin in a solution of 1×10^{-4} M

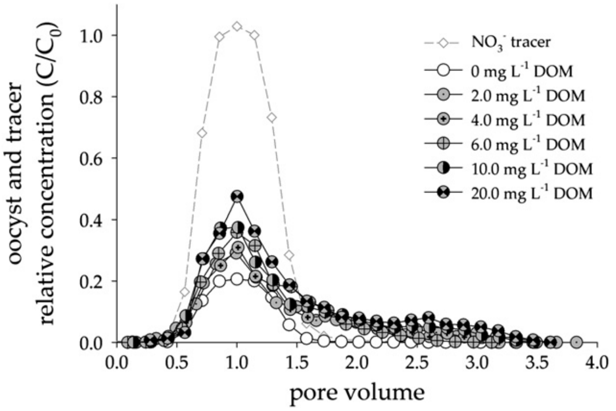

Fig. 3 – Breakthrough curves of the conservative tracer nitrate and the *Cryptosporidium parvum* oocysts as a function of dissolved organic matter concentration in 10^{-4} M NaCl solution at pH 5.6–5.8 in a 4.0% ferric oxyhydroxide-coated sand in the flow-through column. One pore volume is 6.7 mL. The conservative tracer breakthrough curve is shown for one column experiment. Duplicate experiments are not shown.

NaCl and pH 5.6–5.8 without dissolved organic matter was within the range of zeta potentials measured in similar solutions for active, heat-inactivated, and formalin-inactivated oocysts in similar solutions (Drozd and Schwartzbrod, 1996; Brush et al., 1998; Karaman et al., 1999; Considine et al., 2002; Hsu and Huang, 2002; Butkus et al., 2003; Kuznar and Elimelech, 2005).

The addition of dissolved organic matter to the oocyst suspension resulted in more negative zeta potential by only 1 mV, an insignificant change considering the precision of the zeta potential measurement by laser Doppler microelectrophoresis. Other researchers have observed that the addition of organic matter fractions isolated by similar techniques to oocyst suspensions have resulted in significantly more negative oocyst zeta potentials (Ongerth and Pecoraro, 1996; Considine et al., 2002; Dai and Hozalski, 2002, 2003). In distilled water at pH 6.3, the addition of 2.4 mg L^{-1} of a fulvic acid isolated from a forest floor pond made the zeta potential of active oocysts more negative by about 10 mV (Ongerth and Pecoraro, 1996). In a dilute sodium bicarbonate solution at pH 6.7–7.0, the addition of about 10 mg L^{-1} of organic matter from the Suwannee River made the zeta potential of active oocysts more negative by about 20–24 mV (Dai and Hozalski, 2002, 2003). In a 1 mM potassium nitrate solution at pH 6, the addition of about 5–20 mg L^{-1} of organic matter concentration from a reservoir made the zeta potential of active oocysts more negative by about 8–16 mV (Considine et al., 2002). These results certainly suggest that organic matter was interacting with the oocyst surfaces.

For our results, we surmise that our dissolved organic matter, the Everglades F1 fulvic acid, did not interact with our formalin-inactivated oocysts. We did not expect any interaction of dissolved organic matter with oocysts because the oocysts were negatively-charged and the dissolved organic matter would be anionic at the pH values (5.6–5.8) of our experiments.

The differences in the reported effects of dissolved organic matter on oocyst zeta potential might be the result of differences in oocyst inactivation or abundance of polyvalent cations. It is possible that formalin inactivation removes functional groups from oocyst surface proteins, which are composed primarily of cysteine, proline, and histidine (Ranucci et al., 1993), or anchored glycoproteins (Harris and Petry, 1999) with which organic matter might form hydrogen bonds in spite of electrostatic repulsion. We used formalin-inactivated oocysts in these experiments to better understand the transport of oocysts in an intermediate-scale aquifer tank experiment in a laboratory that could not be secured for examination of active oocysts. Dai and Hozalski (2003) suggested that organic matter adsorption to oocysts might be mediated by polyvalent cations (e.g., Ca^{2+}) present in the ash content of the organic matter isolates. Our Everglades fulvic acid had lower ash content than the Suwannee River organic matter used by Dai and Hozalski (2003), but ash content is usually dominated by monovalent, not polyvalent, cations.

4.2. *Effect of organic matter on ferric oxyhydroxide-coated sand surface properties*

The equilibration of the ferric oxyhydroxide-coated sand with dissolved organic matter during the streaming potential measurements resulted in adsorption of organic matter and reversal of surface charge (as measured indirectly by streaming potential) (Fig. 2). Charge reversal occurred at a relatively low concentration of organic matter – somewhere between 0 and 1.9 mg L^{-1}, or about 1 mg L^{-1}, of the Everglades fulvic acid (Fig. 1). Other studies have shown that charge reversal for ferric oxyhydroxide and oxide colloids occur at low concentrations of dissolved organic matter and organic acids of low molecular weight (Liang and Morgan, 1990; Tiller and O'Melia, 1993; Kreller et al., 2003; Kumpulainen et al., 2008). The amount of adsorbed organic matter responsible for charge reversal was about 0.03 mg m^{-2} (based on an assumed surface area of 50 m^2 g^{-1} for the ferric oxyhydroxide). At an acidic functional group content of 6.9 meq g^{-1} for the Everglades fulvic acid, the adsorbed surface charge density is about 2×10^{-7} eq m^{-2} of ferric oxyhydroxide coating. The positive surface charge density of goethite, a common ferric oxyhydroxide, at a pH of about 5.6–5.8 and extrapolated to an ionic strength of 10^{-4} M is about 1–6 $\times 10^{-7}$ eq m^{-2} (Atkinson et al., 1967; Zeltner and Anderson, 1988); therefore, the negative charge on the adsorbed organic matter is about equal to the expected positive charge on the ferric oxyhydroxide coating.

As the organic matter adsorption density increased, the zeta potential (measured as streaming potential) of the ferric oxyhydroxide-coated sand continued to become more negative until the zeta potential reached a plateau of about −70 mV at an organic matter adsorption density of about 0.7 mg m^{-2}, or about 5×10^{-6} eq m^{-2} of charge. The maximum adsorption density was achieved at dissolved organic matter concentrations of 11.1 and 17.3 mg L^{-1}. Ferric oxyhydroxides can adsorb organic matter in excess of their surface charge through specific complexation between organic matter functional groups and surface iron (Gu et al., 1994). Because the ferric oxyhydroxide coatings in the flow-through columns were exposed to the same amount of dissolved organic matter as the ferric oxyhydroxide coatings in the streaming potential cells (normalized for the mass of grains and the surface coatings of 4% for the column and 75% for the cell), the zeta potentials and adsorption densities measured by streaming potential are expected to be relevant for the flow-through columns.

4.3. Effect of dissolved organic matter on oocyst transport

The transport of oocysts through the ferric oxyhydroxide-coated quartz sand increased as the concentration of dissolved organic matter increased (Fig. 3). Similar results have been observed for in laboratory columns and in field experiments for colloids and microbes in geochemically heterogeneous porous media (Fuhs et al., 1985; Scholl and Harvey, 1992; Kretzschmar et al., 1995; Pieper et al., 1997; Ryan et al., 1999; Dong et al., 2002). Based on our results, we can assert that the increase in oocyst transport can be attributed to adsorption of dissolved organic matter to the ferric oxyhydroxide coatings, which reduced the ability of those coatings to adhere oocysts. The dissolved organic matter had no significant effect on the surface properties of the oocysts (Fig. 1).

In the absence of organic matter, oocyst collisions with the coated grains resulted in attachment for 26% of the collisions ($\alpha = 0.26$; Fig. 4). The increase in organic matter concentration resulted in a decrease in the collision efficiency to attachment following about 12% of the collisions ($\alpha = 0.12$), nearly a two-fold decrease in collision efficiency for the oocysts. The oocyst breakthrough increased linearly and the collision efficiency decreased linearly with increasing dissolved organic matter concentration until the concentration reached 10 mg L^{-1}. At the highest dissolved organic matter concentration of 20 mg L^{-1}, the breakthrough and collision efficiency appeared to approach a plateau, which correlates well with the plateau observed for the amount of organic matter adsorbed on the ferric oxyhydroxide coatings (Fig. 2).

For reference, the collision efficiency of the quartz sand alone, without ferric oxyhydroxide coating or organic matter, is $\alpha = 0.06$ (Abudalo et al., 2005). With no organic matter present, the collision efficiency of the 4.0% ferric oxyhydroxide-coated sand was $\alpha = 0.26$. The ferric oxyhydroxide coating increased the collision efficiency of the quartz sand from $\alpha = 0.06$ to 0.26, so the ferric oxyhydroxide coating was responsible for 77% of the removal of oocysts with no organic matter present, and the other 23% of the removal of oocysts occurred on the quartz surfaces. At the highest organic matter concentration, the collision efficiency decreased to $\alpha = 0.12$, so the ferric oxyhydroxide coating removed 50% of the oocysts and the quartz surface removed 50% (assuming that organic matter did not adsorb to the quartz surfaces and did not affect interactions of the oocysts with the quartz surfaces). At the highest organic matter concentration (20 mg L^{-1}), the 4.0% of the sand surface coated by ferric oxyhydroxide removed an unexpectedly high 50% of the oocysts. The adsorption of organic matter rendered the ferric oxyhydroxide coatings as negatively-charged as the quartz surface, which was measured at −71 mV in the same background solution (Abudalo, 2006), so we expected that the 4% coatings would remove only 4% of the oocysts, not 50%. We know that zeta potential is not a good measure of colloid removal for geochemically heterogeneous porous media (Elimelech et al., 2000). It is possible that the adsorption of organic matter to the ferric oxyhydroxide coatings is patchy like the coatings of ferric oxyhydroxide on the quartz sand are patchy, and oocysts are still able to find ferric oxyhydroxide surface area to which organic matter is not adsorbed.

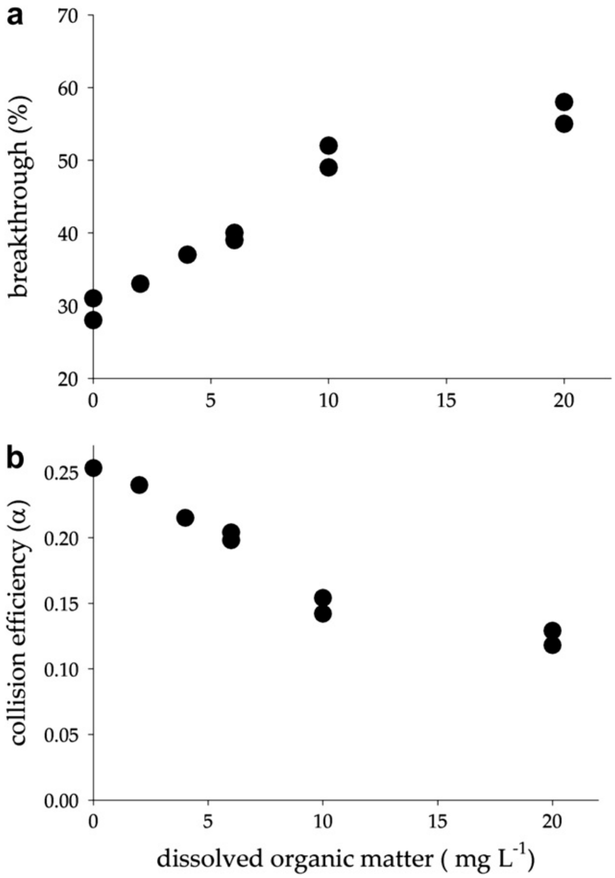

Fig. 4 – Relative breakthrough (a); and collision efficiency (b) of the *Cryptosporidium parvum* oocysts as a function of dissolved organic matter concentration in 10^{-4} M NaCl solution at pH 5.6–5.8 in a 4.0% ferric oxyhydroxide-coated sand in the flow-through column.

The uncoated quartz sand is capable of removing oocysts at the relatively high collision efficiency of $\alpha = 0.06$ (Abudalo et al., 2005). Both the oocysts and quartz are negatively-charged at the pH of these experiments (5.6–5.8). Electrostatic repulsion, and also some steric hindrance (Considine et al., 2001; Kuznar and Elimelech, 2005), should result in minimal attachment. We were concerned that physical straining might be responsible for some of the oocyst removal in these experiments. The median grain size of the well-sorted, well-rounded sand used for these experiments was 0.92 mm, which results in a ratio of oocyst diameter to grain diameter of $d_o/d_g = 0.0039$. This ratio is just above the ratio of 0.0017 for which Bradford et al. (2002) advised that straining may be contributing to removal, but substantially below the ratio of 0.016 for which Tufenkji et al. (2004) did not observe straining of oocysts in a porous medium of spherical glass beads. Owing to the relatively low zeta potentials of oocysts, removal to

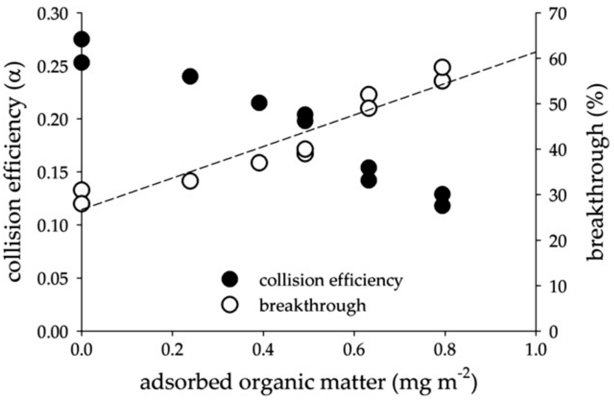

Fig. 5 – Collision efficiency and relative breakthrough of the *Cryptosporidium parvum* oocysts as a function of adsorbed organic matter density. The adsorbed organic matter densities were calculated assuming that the surface area of the ferric oxyhydroxide coating is 50 m^2 g^{-1}. The linear regression (dashed line) for the dependence of the breakthrough (*B*) on the adsorbed organic matter density ($[DOM]_{ads}$) is $B = 35(\pm4)\ [DOM]_{ads} + 27(\pm2)$.

quartz has been attributed to deposition in the secondary minimum of the double layer-van der Waals energy profile for oocyst-quartz interactions (Liu et al., 2009). Removal of oocysts attributed to deposition on the quartz surfaces may include oocyst straining and secondary minimum deposition to the quartz surfaces. The tailing observed in our oocyst breakthrough curves may be attributed to release of oocysts weakly deposited in the secondary minimum.

The oocyst breakthrough increased and the collision efficiency decreased as the concentration of adsorbed organic matter increased (Fig. 5). The adsorbed organic matter concentrations were estimated for the dissolved organic matter concentrations used in the flow-through column experiment using the Langmuir isotherm fit to the adsorption data from the streaming potential measurement (Fig. 2a). The slope of the linear regression of the breakthrough versus the adsorbed organic matter concentration gives slope of 35 ± 4% per (mg m^{-2}). For the flow-through column experiments, a 5.0 mL volume of oocysts were injected at a concentration of 4×10^5 oocysts mL^{-1}. The total number of oocysts injected was 2×10^6 and 35% of the total is 7×10^5 oocysts, so the slope can be re-stated at 7×10^5 oocysts per (mg m^{-2}) of adsorbed organic matter. This slope represents the number of oocysts prevented from attaching to the ferric oxyhydroxide coating by adsorption of an amount of organic matter. A milligram of our dissolved organic matter, the Everglades fulvic acid with a molecular weight of 850 Da, is 7×10^{17} molecules; therefore, the deposition of each oocyst is blocked by the adsorption of about 1×10^{12} molecules of the Everglades fulvic acid.

5. Conclusions

We examined the effect of dissolved organic matter on the transport of *Cryptosporidium parvum* oocysts in a saturated porous medium of ferric oxyhydroxide-coated quartz and found that organic matter enhances the transport of the oocysts. To better understand the mechanism of the effect of dissolved organic matter on oocyst transport, we examined the surface properties of the oocysts and the ferric oxyhydroxide-coated sand as a function of dissolved organic matter concentration. Microelectrophoresis showed that the dissolved organic matter had no significant effect on the zeta potential of the oocysts. Streaming potential measurements showed that even a small amount of organic matter (about 1 mg L^{-1}) was capable of reversing the surface charge of the ferric oxyhydroxide-coated sand from positive to negative. We measured the amount of organic matter adsorbed to the ferric oxyhydroxide-coated sand and found that zeta potentials measured for the ferric oxyhydroxide-coated sand became more negative as the adsorbed organic matter density increased. The results showed that organic matter enhances the transport of oocysts by reducing the ability of the ferric oxyhydroxide coating to promote oocyst attachment through electrostatic attraction.

Our results indicate that low concentrations of dissolved organic matter in solution are likely in equilibrium with sufficient adsorbed organic matter to enhance the transport of *Cryptosporidium parvum* oocysts in geochemically heterogeneous porous media like that encountered in bank filtration. Bank filtration will typically draw in surface water with dissolved organic matter in excess of the 2 mg L^{-1} concentration that caused charge reversal of the ferric oxyhydroxide-coated quartz grains and allowed greater oocyst transport.

Acknowledgments

This research was supported by the U.S. Environmental Protection Agency (STAR grants R826179010 and R829010010). The authors thank George Aiken (U.S. Geological Survey) for the Florida Everglades fulvic acid sample.

REFERENCES

Abudalo, R.A., 2006. Evaluation of the Effect of Geochemical and Physical Heterogeneity on *Cryptosporidium parvum* Oocyst Transport in Saturated Porous Media. PhD thesis, University of Colorado at Boulder, Boulder, CO.

Abudalo, R.A., Bogatsu, Y.G., Ryan, J.N., Harvey, R.W., Metge, D.W., Elimelech, M., 2005. Effect of ferric oxyhydroxide grain coatings on the transport of bacteriophage PRD1 and *Cryptosporidium parvum* oocysts in saturated porous media. Environmental Science and Technology 39, 6412–6419.

Aiken, G.R., McKnight, D.M., Thorn, K.A., Thurman, E.M., 1992. Isolation of hydrophilic organic acids from water using nonionic macroporous resins. Organic Geochemistry 18, 567–573.

Amelung, W., Kaiser, K., Kammerer, G., Sauer, G., 2002. Organic carbon at soil particle surfaces – evidence from X-ray photoelectron spectroscopy and surface abrasion. Soil Science Society of America Journal 66, 1526–1530.

Amirbahman, A., Olson, T.M., 1993. Transport of humic matter-coated hematite in packed beds. Environmental Science and Technology 27, 2807–2813.

Atkinson, R.J., Posner, A.M., Quirk, J.P., 1967. Adsorption of potential-determining ions at the ferric oxide-aqueous electrolyte interface. Journal of Physical Chemistry 71, 550–558.

Bixby, R.L., O'Brien, D.J., 1979. Influence of fulvic acid on bacteriophage adsorption and complexation in soil. Applied and Environmental Microbiology 38, 840–845.

Bradford, S.A., Yates, S.R., Bettahar, M., Simunek, J., 2002. Physical factors affecting the transport and fate of colloids in saturated porous media. Water Resources Research 38, doi:10.1029/2002WR001340.

Brush, C.F., Walter, M.F., Anguish, L.J., Ghiorse, W.C., 1998. Influence of pretreatment and experimental conditions on electrophoretic mobility and hydrophobicity of *Cryptosporidium parvum* oocysts. Applied and Environmental Microbiology 64, 4439–4445.

Butkus, M.A., Bays, J.T., Labare, M.P., 2003. Influence of surface characteristics on the stability of *Cryptosporidium parvum* oocysts. Applied and Environmental Microbiology 69, 3819–3825.

Campbell, P.G.C., Twiss, M.R., Wilkinson, K.J., 1997. Accumulation of natural organic matter on the surfaces of living cells: implications for the interaction of toxic solutes with aquatic biota. Canadian Journal of Fisheries and Aquatic Sciences 54, 2543–2554.

Carey, C.M., Lee, H., Trevors, J.T., 2004. Biology, persistence and detection of *Cryptosporidium parvum* and *Cryptosporidium hominis* oocysts. Water Research 38, 818–862.

Considine, R.F., Drummond, C.J., Dixon, D.R., 2001. Force of interaction between a biocolloid and an inorganic oxide: complexity of surface deformation, roughness, and brushlike behavior. Langmuir 17, 6325–6335.

Considine, R.F., Dixon, D.R., Drummond, C.J., 2002. Oocysts of *Cryptosporidium parvum* and model sand surfaces in aqueous solutions: an atomic force microscope (AFM) study. Water Research 36, 3421–3428.

Cosovic, B., Hrsak, D., Vojvodic, V., Krznaric, D., 1996. Transformation of organic matter and bank filtration from a polluted stream. Water Research 30, 2921–2928.

Coston, J.A., Fuller, C.C., Davis, J.A., 1995. Pb^{2+} and Zn^{2+} adsorption by a natural aluminum- and iron-bearing surface coating on an aquifer sand. Geochimica et Cosmochimica Acta 59, 3535–3547.

Dai, X., Hozalski, R.M., 2002. Effect of nom and biofilm on the removal of *Cryptosporidium parvum* oocysts in rapid filters. Water Research 36, 3523–3532.

Dai, X., Hozalski, R.M., 2003. Evaluation of microspheres as surrogates for *Cryptosporidium parvum* oocysts in filtration experiments. Environmental Science and Technology 37, 1037–1042.

Davis, J.A., 1982. Adsorption of natural dissolved organic matter at the oxide/water interface. Geochimica et Cosmochimica Acta 46, 2381–2393.

Dong, H., Onstott, T.C., Ko, C.H., Hollingsworth, A.D., Brown, D.G., Mailloux, B.J., 2002. Theoretical prediction of collision efficiency between adhesion-deficient bacteria and sediment grain surface. Colloids and Surfaces B: Biointerfaces 24, 229–245.

Drozd, C., Schwartzbrod, J., 1996. Hydrophobic and electrostatic cell surface properties of *Cryptosporidium parvum*. Applied and Environmental Microbiology 62, 1227–1232.

Elimelech, M., Gregory, J., Jia, X., Williams, R. (1995) Particle Deposition & Aggregation. Measurement, Modelling and Simulation, Butterworth-Heinemann, Oxford, England.

Elimelech, M., Nagai, M., Ko, C.H., Ryan, J.N., 2000. Relative insignificance of mineral grain zeta potential to colloid transport in geochemically heterogeneous porous media. Environmental Science and Technology 34, 2143–2148.

Fein, J.B., Boily, J.F., Guclu, K., Kaulbach, E., 1999. Experimental study of humic acid adsorption onto bacteria and Al-oxide mineral surfaces. Chemical Geology 162 (1), 33–45.

Foppen, J.W.A., Schijven, J.F., 2005. Transport of *E. coli* in columns of geochemically heterogeneous sediment. Water Research 39, 3082–3088.

Franchi, A., O'Melia, C.R., 2003. Effects of natural organic matter and solution chemistry on the deposition and reentrainment of colloids in porous media. Environmental Science and Technology 37, 1122–1129.

Fuhs, G.W., Chen, M., Sturman, L.S., Moore, R.S., 1985. Virus adsorption to mineral surfaces is reduced by microbial overgrowth and organic coatings. Microbial Ecology 11, 25–39.

Gollnitz, W.D., Clancy, J.L., Whitteberry, B.L., Vogt, J.A., 2003. RBF as a microbial treatment process. Journal of the American Water Works Association 95, 56–66.

Grünheid, S., Amy, G., Jekel, M., 2005. Removal of bulk dissolved organic carbon (DOC) and trace organic compounds by bank filtration and artificial recharge. Water Research 39, 3219–3228.

Gu, B., Schmitt, J., Chen, Z., Liang, L., McCarthy, J.F., 1994. Adsorption and desorption of natural organic matter on iron oxide: mechanisms and models. Environmental Science and Technology 28, 38–46.

Hall, J.A., Mailloux, B.J., Onstott, T.C., Scheibe, T.D., Fuller, M.E., Dong, H., DeFlaun, M.F., 2005. Physical versus chemical effects on bacterial and bromide transport as determined from on site sediment column pulse experiments. Journal of Contaminant Hydrology 76, 295–314.

Harris, J.R., Petry, F., 1999. *Cryptosporidium parvum*: structural components of the oocyst wall. The Journal of Parasitology 85 (5), 839–849.

Harvey, R.W., Garabedian, S.P., 1991. Use of colloid filtration theory in modeling movement of bacteria through a contaminated sandy aquifer. Environmental Science and Technology 25, 178–185.

Harvey, R.W., Metge, D.W., Kinner, N., Mayberry, N., 1997. Physiological considerations in applying laboratory-determined buoyant densities to predictions of bacterial and protozoan transport in groundwater: results of in-situ and laboratory tests. Environmental Science and Technology 31, 289–295.

Hijnen, W.A.M., Brouwer-Hanzens, A.J., Charles, K.J., Medema, G.J., 2005. Transport of MS2 phage, *Escherichia coli, Clostridium perfringens, Cryptosporidium parvum*, and *Giardia intestinalis* in a gravel and a sandy soil. Environmental Science and Technology 39, 7860–7868.

Hsu, B.M., Huang, C., 2002. Influence of ionic strength and pH on hydrophobicity and zeta potential of *Giardia* and *Cryptosporidium*. Colloids and Surfaces A: Physicochemical and Engineering Aspects 201, 201–206.

Johnson, P.R., 1999. A comparison of streaming and microelectrophoresis methods for obtaining the ζ potential of granular porous media surfaces. Journal of Colloid and Interface Science 209, 264–267.

Johnson, W.P., Logan, B.E., 1996. Enhanced transport of bacteria in porous media by sediment-phase and aqueous-phase organic matter. Water Research 30, 923–931.

Johnson, P.R., Sun, N., Elimelech, M., 1996. Colloid transport in geochemically heterogeneous porous media: modeling and measurements. Environmental Science and Technology 30, 3284–3293.

Karaman, M.E., Pashley, R.M., Bustamante, H., Shanker, S.R., 1999. Microelectrophoresis of *Cryptosporidium parvum* oocysts in aqueous solutions of inorganic and surfactant cations. Colloids and Surfaces A: Physicochemical and Engineering Aspects 146, 217–225.

Kim, S.-B., Park, S.-J., Lee, C.-G., Kim, H.-C., 2008. Transport and retention of *Escherichia coli* in a mixture of quartz, Al-coated and Fe-coated sands. Hydrological Processes 22 (18), 3856–3863.

Kreller, D.I., Gibson, G., Novak, W., Van Loon, G.W., Horton, J.H., 2003. Competitive adsorption of phosphate and carboxylate with natural organic matter on hydrous iron oxides as investigated by chemical force microscopy. Colloids and Surfaces A: Physicochemical and Engineering Aspects 212, 249–264.

Kretzschmar, R., Robarge, W.P., Amoozegar, A., 1995. Influence of natural organic matter on colloid transport through saprolite. Water Resources Research 31, 435–445.

Kumpulainen, S., von der Kammer, F., Hofmann, T., 2008. Humic acid adsorption and surface charge effects on schwertmannite and goethite in acid sulphate waters. Water Research 42, 2051–2060.

Kuznar, Z.A., Elimelech, M., 2005. Role of surface proteins in the deposition kinetics of *Cryptosporidium parvum* oocysts. Langmuir 21, 710–716.

Levy, J., Sun, K., Findlay, R.H., Farruggia, F.T., Porter, J., Mumy, K.L., Tomaras, J., Tomaras, A., 2007. Transport of *Escherichia coli* bacteria through laboratory columns of glacial-outwash sediments: estimating model parameter values based on sediment characteristics. Journal of Contaminant Hydrology 89, 71–106.

Liang, L., Morgan, J.J., 1990. Chemical aspects of iron oxide coagulation in water: laboratory studies and implications for natural systems. Aquatic Sciences 52, 32–55.

Liu, Y., Janjaroen, D., Kuhlenschmidt, M.S., Kuhlenschmidt, T.B., Nguyen, T.H., 2009. Deposition of *Cryptosporidium parvum* oocysts on natural organic matter surfaces: microscopic evidence for secondary minimum deposition in a radial stagnation point flow cell. Langmuir 25 (3), 1594–1605.

MacKenzie, W.R., Hoxie, N.J., Proctor, M.E., Gradus, M.S., Blair, K.A., Peterson, D.E., Kazmierczak, J.J., Addiss, D.G., Fox, K.R., Rose, J.B., Davis, J.P., 1994. A massive outbreak in Milwaukee of *Cryptosporidium* infection transmitted through the public water supply. New England Journal of Medicine 331, 161–167.

Martin, R.E., Hanna, L.M., Bouwer, E.J., 1991. Determination of bacterial collision efficiencies in rotating disk system. Environmental Science and Technology 25, 1068–1074.

Medema, G.J., Schets, F.M., Teunis, P.F.M., Havelaar, A.H., 1998. Sedimentation of free and attached *Cryptosporidium* oocysts and *Giardia* cysts in water. Applied and Environmental Microbiology 64 4469–4466.

Meier, M., Namjesnik-Dejanovic, K., Maurice, P.A., Chin, Y.P., Aiken, G.R., 1999. Fractionation of aquatic natural organic matter upon sorption to goethite and kaolinite. Chemical Geology 157, 275–284.

Miettinen, I.T., Martikainen, P.J., Vartiainen, T., 1994. Humus transformation at the bank filtration water-plant. Water Science and Technology 30, 179–187.

Mills, A.L., Herman, J.S., Hornberger, G.M., DeJesus, T.H., 1994. Effect of solution ionic strength and iron coatings on minerals grains on the sorption of bacterial cells to quartz sand. Applied and Environmental Microbiology 60, 3300–3306.

Ongerth, J.E., Pecoraro, J.P., 1996. Electrophoretic mobility of *Cryptosporidium* oocysts and *Giardia* cysts. Journal of Environmental Engineering 122, 228–231.

Parent, M.E., Velegol, D., 2004. *E. coli* adhesion to silica in the presence of humic acid. Colloids and Surfaces B: Biointerfaces 39, 45–51.

Penn, R.L., Zhu, C., Xu, H., Veblen, D.R., 2003. Iron oxide coatings on sand grains from the Atlantic coastal plain: high-resolution transmission electron microscopy characterization. Geology 29, 843–946.

Pieper, A.P., Ryan, J.N., Harvey, R.W., Amy, G.L., Illangasekare, T.H., Metge, D.W., 1997. Transport and recovery of bacteriophage PRD1 in a sand and gravel aquifer: effect of sewage-derived organic matter. Environmental Science and Technology 31, 1163–1170.

Powelson, D.K., Simpson, J.R., Gerba, C.P., 1990. Virus transport and survival in saturated and unsaturated flow through soil columns. Journal of Environmental Quality 19, 396–401.

Ranucci, L., Muller, H.M., Larosa, G., Reckmann, I., Morales, M.A.G., Spano, F., Pozio, E., Crisanti, A., 1993. Characterization and immunolocalization of a *Cryptosporidium* protein containing repeated amino-acid motifs. Infection and Immunity 61, 2347–2356.

Ravichandran, M., Aiken, G.R., Reddy, M.M., Ryan, J.N., 1998. Enhanced dissolution of cinnabar (mercuric sulfide) by dissolved organic matter isolated from the Florida Everglades. Environmental Science and Technology 32, 3305–3311.

Redman, J.A., Grant, S.B., Olson, T.M., Hardy, M.E., Estes, M.K., 1997. Filtration of recombinant Norwalk virus particles and bacteriophage MS2 in quartz sand: importance of electrostatic interactions. Environmental Science and Technology 31, 3378–3383.

Ryan, J.N., Gschwend, P.M., 1992. Effect of iron diagenesis on the transport of colloidal clay in an unconfined sand aquifer. Geochimica et Cosmochimica Acta 56, 1507–1521.

Ryan, J.N., Elimelech, M., Ard, R.A., Harvey, R.W., Johnson, P.R., 1999. Bacteriophage PRD1 and silica colloid transport and recovery in an iron oxide-coated sand aquifer. Environmental Science and Technology 33, 63–73.

Scholl, M.A., Harvey, R.W., 1992. Laboratory investigations on the role of sediment surface and groundwater chemistry in transport of bacteria through a contaminated sandy aquifer. Environmental Science and Technology 26, 1410–1417.

Schwertmann, U., Cornell, R.M. (2003) The Iron Oxides: Structure, Properties, Reactions, Occurrences and Uses, Wiley-VCH GmbH & Co. KGaA, Weinheim, Germay.

Song, L., Johnson, P.R., Elimelech, M., 1994. Kinetics of colloid deposition onto heterogeneously charged surfaces in porous media. Environmental Science and Technology 28, 1164–1171.

Tiller, C.L., O'Melia, C.R., 1993. Natural organic-matter and colloidal stability – models and measurements. Colloids and Surfaces A: Physicochemical and Engineering Aspects 73, 89–102.

Tufenkji, N., Elimelech, M., 2004. Correlation equation for predicting single-collector efficiency in physicochemical filtration in saturated porous media. Environmental Science and Technology 38, 529–536.

Tufenkji, N., Ryan, J.N., Elimelech, M., 2002. The promise of bank filtration. Environmental Science and Technology 36, A422–A428.

Tufenkji, N., Miller, G.F., Ryan, J.N., Harvey, R.W., Elimelech, M., 2004. Transport of *Cryptosporidium* oocysts in porous media: role of straining and physicochemical filtration. Environmental Science and Technology 38, 5932–5938.

Wagai, R., Mayer, L.M., Kitayama, K., 2009. Extent and nature of organic coverage of soil mineral surfaces assessed by a gas sorption approach. Geoderma 149 (1–2), 152–160.

Yuan, B., Pham, M., Nguyen, T.H., 2008. Deposition kinetics of bacteriophage MS2 on a silica surface coated with natural organic matter in a radial stagnation point flow cell. Environmental Science and Technology 42 (20), 7628–7633.

Zeltner, W.A., Anderson, M.A., 1988. Surface charge development at the goethite/aqueous solution interface: effects of CO_2 adsorption. Langmuir 4, 469–474.

Zhuang, J., Jin, Y., 2003a. Virus retention and transport as influenced by different forms of soil organic matter. Journal of Environmental Quality 32, 816–823.

Zhuang, J., Jin, Y., 2003b. Virus retention and transport through Al-oxide coated sand columns: effects of ionic strength and composition. Journal of Contaminant Hydrology 60, 193–209.